Asian Journal of Civil Engineering
https://doi.org/10.1007/s42107-023-00886-w

RESEARCH

Machine learning models for predicting the axial compression capacity of cold-formed steel elliptical hollow section columns

Trong-Ha Nguyen[1] · Duc-Xuan Nguyen[1] · Thanh-Tung Thi Nguyen[1] · Van-Long Phan[1] · Duy-Duan Nguyen[1]

Received: 11 August 2023 / Accepted: 23 August 2023

Abstract

This study presents the performance of three machine learning (ML) models including gradient boosting regression trees (GBRT), artificial neural network model (ANN), and artificial neural network–particle swarm optimization (ANN-PSO) for predicting the axial compression capacity (ACC) of cold-formed steel elliptical hollow section (EHS) columns. To achieve the goal, a set of 291 data is collected from previous studies to develop GBRT, ANN, and ANN-PSO models. The performance of GBRT, ANN, and ANN-PSO models is evaluated based on the statistical indicators, which are R^2, RMSE, MAPE, and $i20-\text{index}$. The results show that the ANN-PSO model with $R^2 = 1.00, \text{RMSE} = 41.3631, \text{MAPE} = 1.3689$, and $i20-\text{index} = 0.9966$ has the best performance compared to GBRT and ANN models. Moreover, a graphical user interface tool is developed based on the ANN-PSO model for practical designs.

Keywords Artificial neural network model · Gradient boosting regression trees · Artificial neural network–particle swarm optimization · Cold-formed steel elliptical hollow section · Axial compression capacity

Introduction

The cold-formed steel elliptical hollow section (EHS) is a special geometric property since it has major and minor axes, as shown in Fig. 1. This allows the designer to make a reasonable selection between the loading resistance and economical use of materials. However, the design process of EHS members has not been specified clearly in current design codes such as Eurocode 3 (1993-3-1, 2006), ANSI/AISC360 (ANSI/AISC360, 2016) or AISI-S100 (AISI-S100, 2016). Thus, this has motivated researchers to investigate structural behaviors of EHS members (Chan & Gardner, 2009; Chen & Young, 2019a, 2019b, 2019c, 2020; Law & Gardner, 2013; Mohammed & Cashell, 2021; Theofanous et al., 2009; Yao et al., 2019).

So far, numerous studies were conducted to consider the behaviors of cold-formed steel EHS structures (Chan & Gardner, 2009; Chen & Young, 2019a, 2019c, 2020; Law & Gardner, 2013; Mohammed & Cashell, 2021; Theofanous et al., 2009; Yao et al., 2019). Specifically, studies on axial compression capacity of EHS columns (Chen & Young, 2019c), structural response of steel oval hollow members (Chen & Young, 2019b; Theofanous et al., 2009; Yao et al., 2019), beam-column tests of EHS (Chen & Young, 2020), flexural buckling of EHS columns (Chan & Gardner, 2009), bending behaviors of elliptical sections (Chen & Young, 2019a), global instability of EHS under biaxial bending (Law & Gardner, 2013), and distortional buckling of elliptical tubes (Dias & Silvestre, 2011) were systematically performed. However, it is necessary to develop a tool that can rapidly predict the axial compression capacity (ACC) of EHS columns.

In recent years, machine learning (ML) algorithms have been widely used in engineering problems, especially to estimate the structural responses (Dias & Silvestre, 2011; Kaveh, 2014; Kaveh & Bondarabady, 2004; Kaveh et al., 2008; Naser et al., 2021; Patel & Mehta, 2018; Tran et al.,

✉ Duy-Duan Nguyen
duan468@gmail.com

Trong-Ha Nguyen
trongha@vinhuni.edu.vn

Duc-Xuan Nguyen
ducxuankxd@vinhuni.edu.vn

Thanh-Tung Thi Nguyen
ntttung@gmail.com

Van-Long Phan
phanlongkxd@vinhuni.edu.vn

[1] Department of Civil Engineering, Vinh University, Vinh 461010, Vietnam

Published online: 14 September 2023

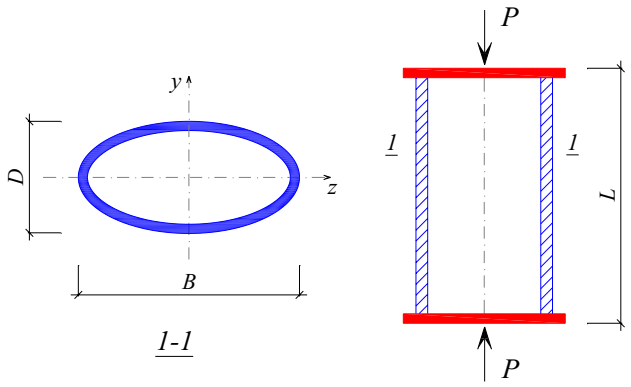

Fig. 1 The EHS column under the axial compression

2019, 2022). Many studies have applied various predicted ML techniques such as gradient boost regression tree (GBRT) (Friedman, 2001; Hao et al., 2022; Manna et al., 2017; Nguyen & Nguyen, 2023; Qi et al., 2018), artificial neural networks (ANNs) (Manna et al., 2017; Nguyen et al., 2023; Rönnholm et al., 2005; Tran et al., 2019, 2022), and other hybrid optimization models (Alizamir & Sobhanardakani, 2018; Kumar et al., 2022; Shariati et al., 2019; Soltani et al., 2022; Toghyani et al., 2016). In addition, comparisons of the prediction performance of ML models were presented (Alzoubi et al., 2018; Le et al., 2019; Liu et al., 2021; Tran & Kim, 2020). However, an evaluation of GBRT, ANN, and artificial neural network–particle swarm optimization (ANN-PSO) models in predicting ACC of cold-formed steel EHS columns is not considered so far.

This study aims to develop three ML models including GBRT, ANN, and ANN-PSO for predicting ACC of cold-formed steel EHS columns. A set of 291 data, consisting of the larger outer diameter (B), smaller outer diameter (D), thickness (t), column length (L), Young's modulus (E), static ultimate tensile strength (σ_u), tensile strain fracture (ε_u), and static 0.2% proof stress ($\sigma_{0.2}$), is considered as the input variables. Meanwhile, the ACC value of cold-formed EHS columns (P) is the output variable. The predicted performance of GBRT, ANN, and ANN-PSO models is then evaluated using typical statistical indicators, which are goodness of fit (R^2), root mean squared error (RMSE), mean absolute percentage error (MAPE), and $a20-$index. To apply the efficient ML model in practical designs, a new graphical user interface is developed.

Data collection

A set of 291 data considering a wide range of the outer diameter (B), smaller outer diameter (D), thickness (t), column length (L), Young's modulus (E), static ultimate tensile strength (σ_u), tensile strain fracture (ε_u), static 0.2% proof stress ($\sigma_{0.2}$), and the ACC of cold-formed EHS columns (P) is carefully collected from the literature (Chan & Gardner, 2009; Chen & Young, 2019a, 2019b, 2019c, 2020; Law & Gardner, 2013; Mohammed & Cashell, 2021; Theofanous et al., 2009; Yao et al., 2019). The statistical properties are shown in Table 1, and frequencies of input database are shown in Fig. 2. Moreover, the correlation matrix of the dataset is shown in Fig. 3. It can be found that the Pearson's correlation coefficients between pairs of B and D and t and P have a significant correlation, while the other parameters have a weak correlation.

Background of machine learning models

Artificial neural network (ANN)

ANN is one of the ML algorithms, and it is a computational model inspired by the structure and function of the human brain. ANN has been popularly employed in the

Table 1 The statistical properties and range of the dataset

	B (mm)	D (mm)	t (mm)	L (mm)	E (MPa)	σ_u (MPa)	$\sigma_{0.2}$ (MPa)	ε_u (%)	P (kN)
Minimum	86.00	50.00	1.50	171.90	185.00	383.00	236.50	0.07	82.00
Mean	271.42	135.18	7.17	2081.25	212.16	464.36	400.57	3.62	1688.10
Maximum	500.00	250.00	25.00	4000.00	213.40	661.00	532.80	4.80	11,397.60
SD	117.23	61.79	5.75	1153.05	2.67	39.06	33.65	0.62	2027.87
CoV	0.43	0.46	0.80	0.55	0.01	0.08	0.08	0.17	1.20

SD standard deviation, *CoV* coefficient of variation

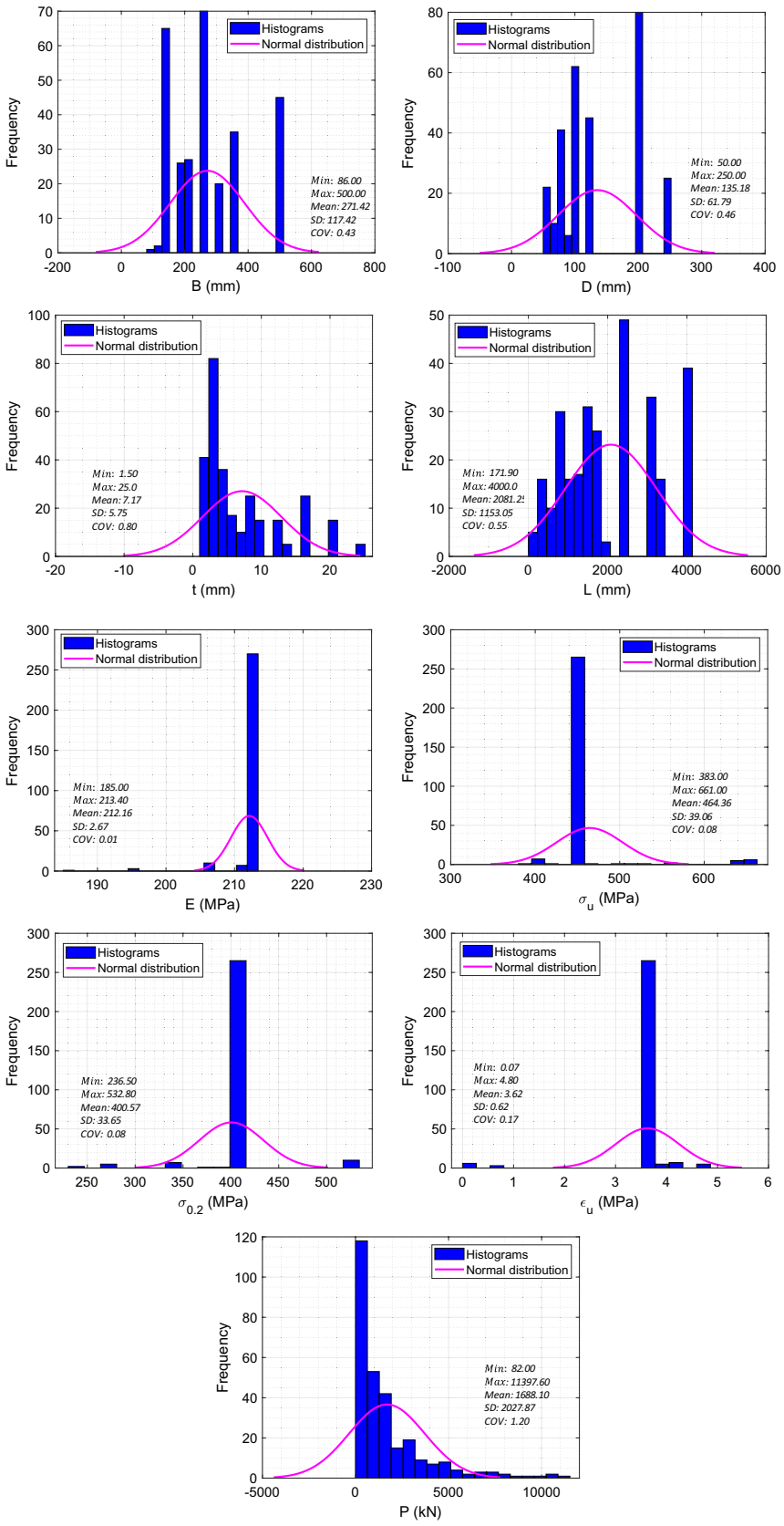

Fig. 2 The statistical characteristics and frequencies of the dataset

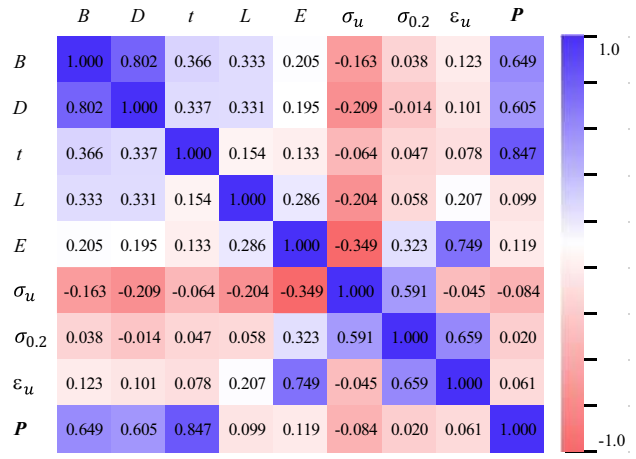

Fig. 3 Correlation matrix of the dataset

civil engineering major (Naser et al., 2021; Tran et al.; Tran et al., 2019). An ANN consists of interconnected nodes, called artificial neurons or "units," organized into layers. The most common type of ANN is the feedforward neural network, where information flows in one direction, from the input layer through one or more hidden layers to the output layer. Each neuron in a layer receives inputs from the previous layer, applies a weighted sum to those inputs, and passes the result through an activation function to produce an output. In this study, the ANN structures used a back-propagation neural network and a Levenberg–Marquardt (L-M) algorithm with a structure of three layers, as shown in Fig. 4. The input layer, hidden layer, and output layer are connected through weights and biases. Its mathematical representation has the form

$$f : \boldsymbol{X} \in R^{D} \rightarrow Y \in R^{1}, \tag{1}$$

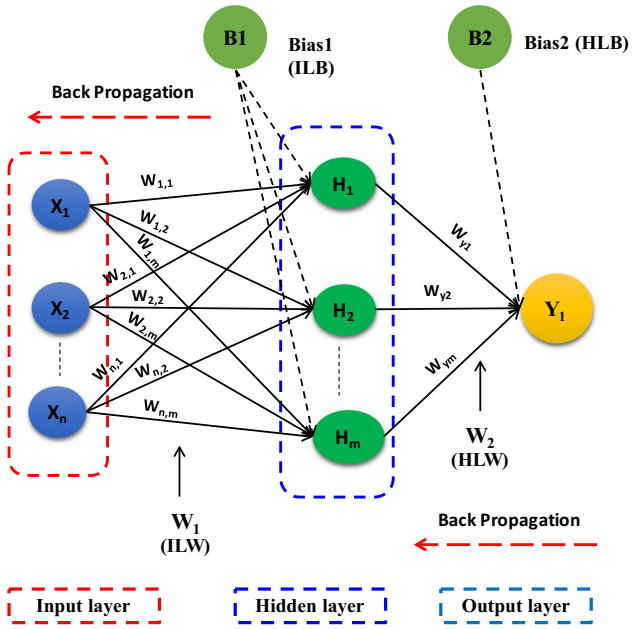

Fig. 4 Illustration of ANN model

$$f(\boldsymbol{X}) = f_0\left(b_2 + W_2 \times \left(f_h\left(b_1 + W_1 \times \boldsymbol{X}\right)\right)\right), \tag{2}$$

where b_1, W_1, and f_h represent the bias, weight, and activation function of the hidden layer, respectively, whereas b_2, W_2, and f_0 are the bias, weight, and activation function of the output layer, respectively.

The nonlinear function (tansig) has been used for the hidden layer activation function and linear function (*purelin*) has been used for the output layer (Nikbin et al., 2017). Its mathematical expression is represented in Eqs. (3–4):

Table 2 Performance of the GBRT, ANN, and ANN-PSO models

Model	R^2	RMSE (kN)	MAPE (%)	*a*20 index	$P_{target}/P_{prediction}$				
					Min	Mean	Max	St.D	CoV
GBRT model									
All data	0.9988	69.86	7.3322	0.9141	0.5772	1.0177	2.1040	0.1445	0.1419
Training	0.9989	65.5810	6.9435	0.9064	0.5772	1.0118	1.8158	0.1347	0.1331
Testing	0.9980	85.5038	8.8835	0.9464	0.8905	1.0430	2.1040	0.1788	0.1715
ANN model									
All data	0.9846	41.4337	28.4896	0.6048	0.2815	1.0759	7.5511	0.6093	0.5664
Training	0.9845	41.2368	31.5565	0.5784	0.2815	1.1300	7.5511	0.6856	0.6067
Testing	0.9358	31.4530	30.6033	0.5238	0.3825	0.9862	2.7003	0.4353	0.4414
ANN-PSO model									
All data	1.000	41.3631	1.3689	0.9966	0.9808	0.9890	1.3882	0.0236	0.0239
Training	1.000	41.1693	1.4281	0.9951	0.9808	0.9896	1.3882	0.0281	0.0284
Testing	1.000	31.1362	1.1583	1.0000	0.9858	0.9884	0.9977	0.0026	0.0026

$$\text{tansig}(x) = \frac{2}{(1 + epx(-2x))} - 1, \tag{3}$$

$$\text{purelin}(x) = x, \tag{4}$$

Continuous feedback loops are performed in the training process. The training process stops through the mean square error index (MSE). The mathematical expression defining MSE is represented as follows:

$$\text{MSE} = \min_{b_1, b_2, W_1, W_2} \frac{1}{N} \sum_{i=1}^{N} e_i^2, \tag{5}$$

where e_i is the deviation between the actual data and output data; N is the sample number of trained ANN models.

ANN-PSO model

For improving the performance of ANN, the optimization of weights and biases values should be conducted. In fact, there are many different techniques for optimizing weights and biases of the ANN model. The PSO technique emerges as an effective method (Eberhart et al., 2001). It is used to optimize continuous nonlinear functions. Moreover, the PSO technique is easy to use in conjunction with ANN training in MATLAB. The training process of ANN—PSO can be implemented using the following basic steps, and the flowchart is shown in Fig. 5:

1. Collection data
2. Input data
3. Create the ANN structures
4. Configure the ANN
5. Initialize the weights and biases
6. Training using PSO with fitness MSE
7. Update PSO operators
8. Optimum weights and biases
9. Validate ANN structures
10. Use the network.

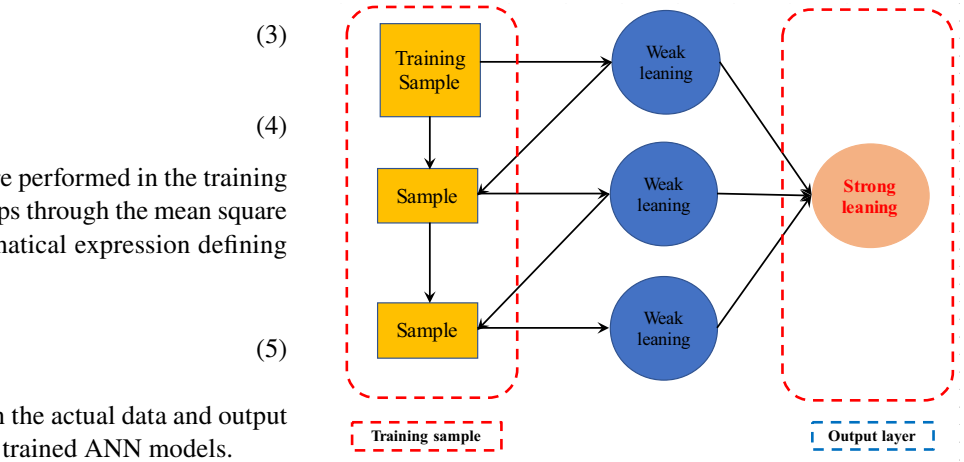

Fig. 6 A typical GBRT model

Gradient boosting regression trees (GBRT)

GBRT is a ML technique that combines multiple decision trees to create a powerful predictive model. It is a popular algorithm for both regression and classification tasks

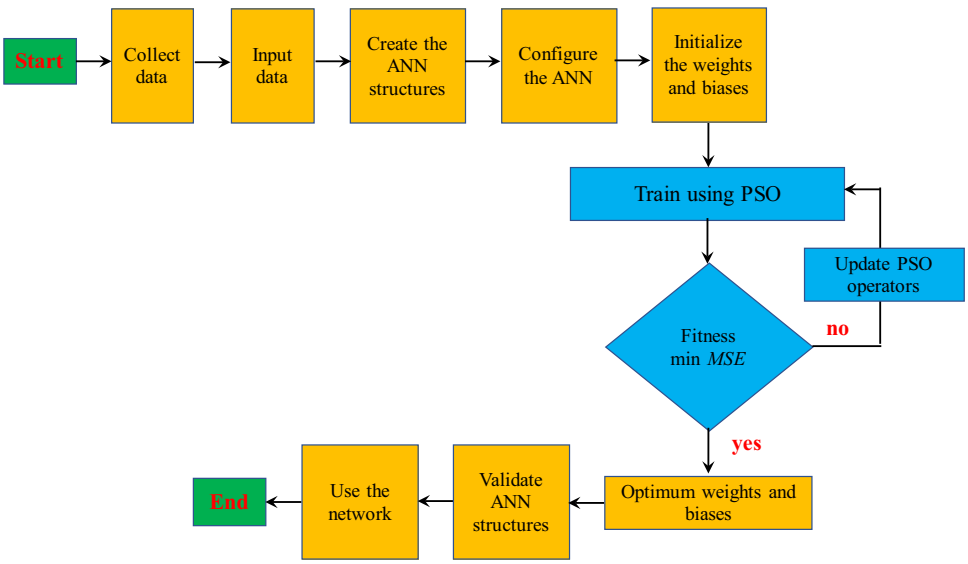

Fig. 5 Flowchart for the training process of the ANN-PSO model

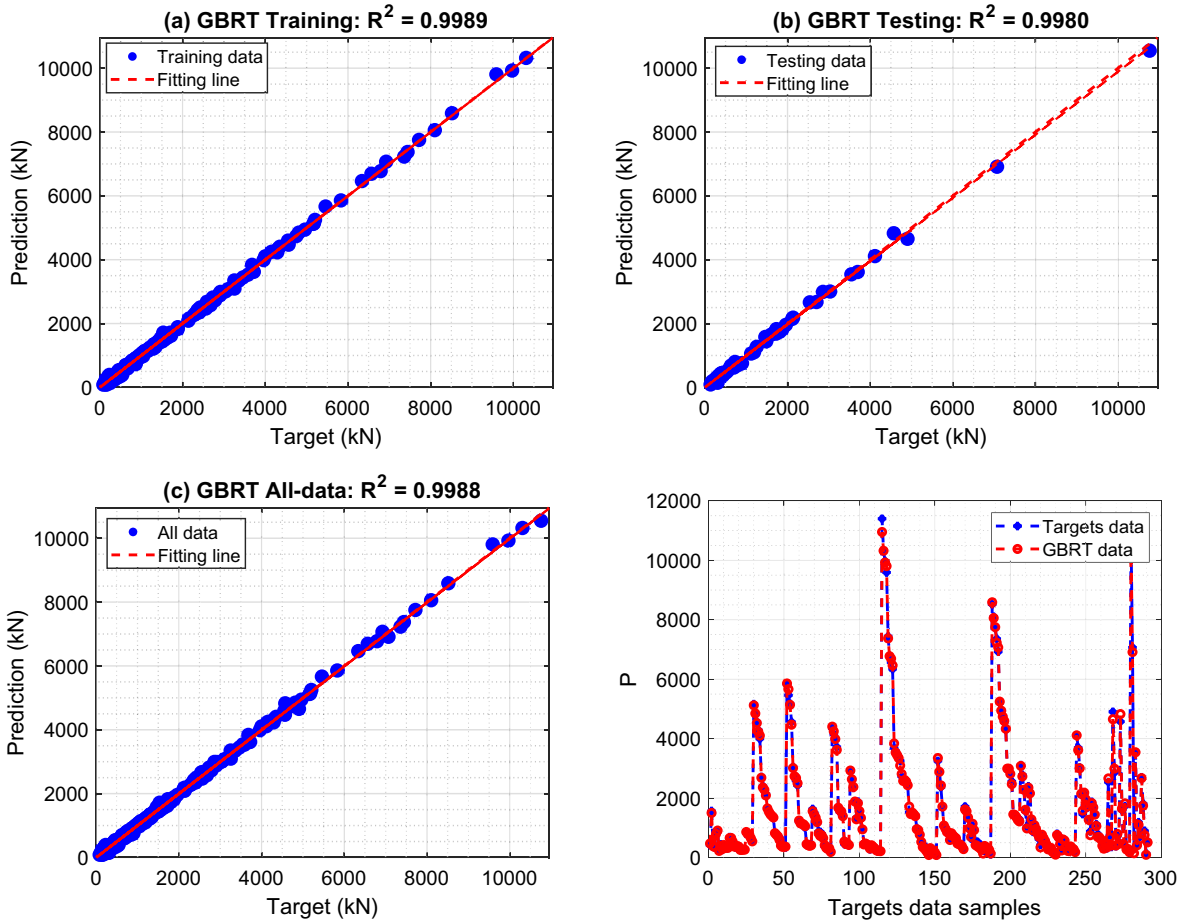

Fig. 7 Performance of GBRT model

Fig. 8 The total ranking matrix of 120 ANN structures

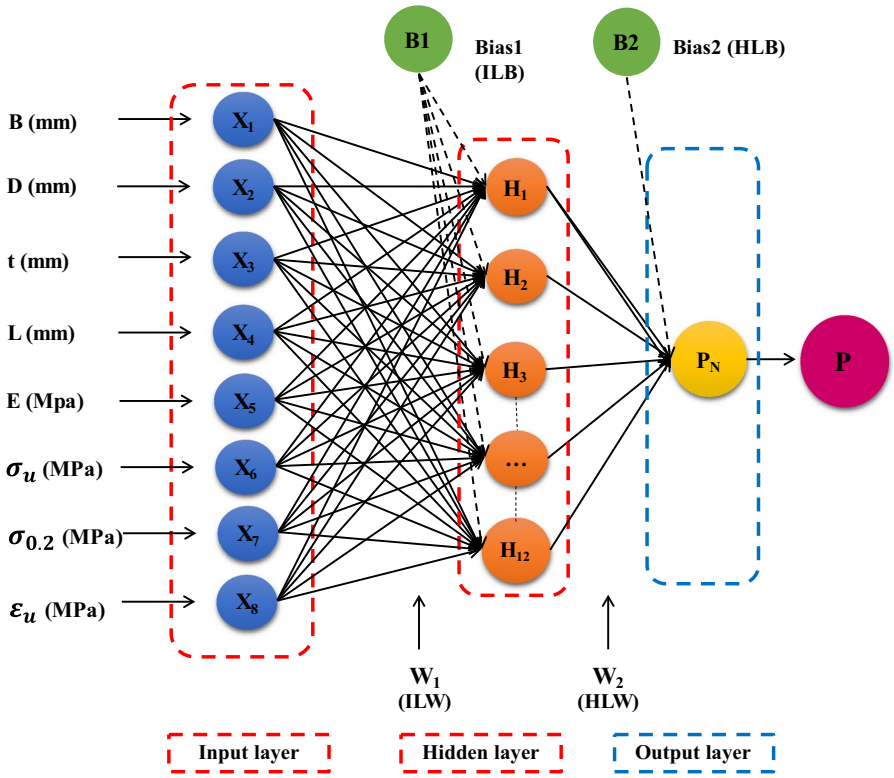

Fig. 9 ANN model structure

(Friedman, 2001; Manna et al., 2017; Nguyen & Nguyen, 2023). Moreover, GBRT combines the strengths of decision trees and boosting to create accurate and robust predictive models. It works by building an ensemble of decision trees sequentially, with each tree learning from the mistakes made by the previous tree. According to Prettenhofer and Louppe (2014), the basic steps for performing GBRT are as follows, and the flowchart is shown in Fig. 6:

1. *Decision trees*: GBRT starts by building an initial decision tree, which is a flowchart-like structure that makes sequential decisions based on the input features. Each decision tree splits the data based on the values of different features, aiming to minimize the prediction error.
2. *Gradient boosting*: GBRT uses a boosting technique called gradient boosting to improve the performance of decision trees. Boosting involves training multiple weak models (in this case, decision trees) sequentially, where each subsequent model focuses on correcting the errors made by the previous models.
3. *Gradient descent*: The "gradient" in GBRT refers to the gradient of the loss function with respect to the model's predictions. GBRT uses gradient descent to optimize the model by iteratively updating the model's predictions to minimize the loss function. The gradient descent process involves calculating the gradients and adjusting the model's predictions in the opposite direction of the gradients.
4. *Weak learners*: GBRT treats decision trees as weak learners because they are simple and prone to overfitting. By combining multiple decision trees, GBRT creates a strong ensemble model that can capture complex relationships in the data.
5. *Ensemble of trees*: GBRT builds an ensemble of decision trees, where each subsequent tree is trained to correct the mistakes made by the previous trees. The final prediction is obtained by aggregating the predictions of all the trees in the ensemble.

Data normalization

The accuracy in training the network depends on the input data normalization (Golafshani & Ashour, 2016). Input data and output data normalized in the range $[-1, 1]$. Before training the network, the input and output data must be data normalized according to the Eq. (9):

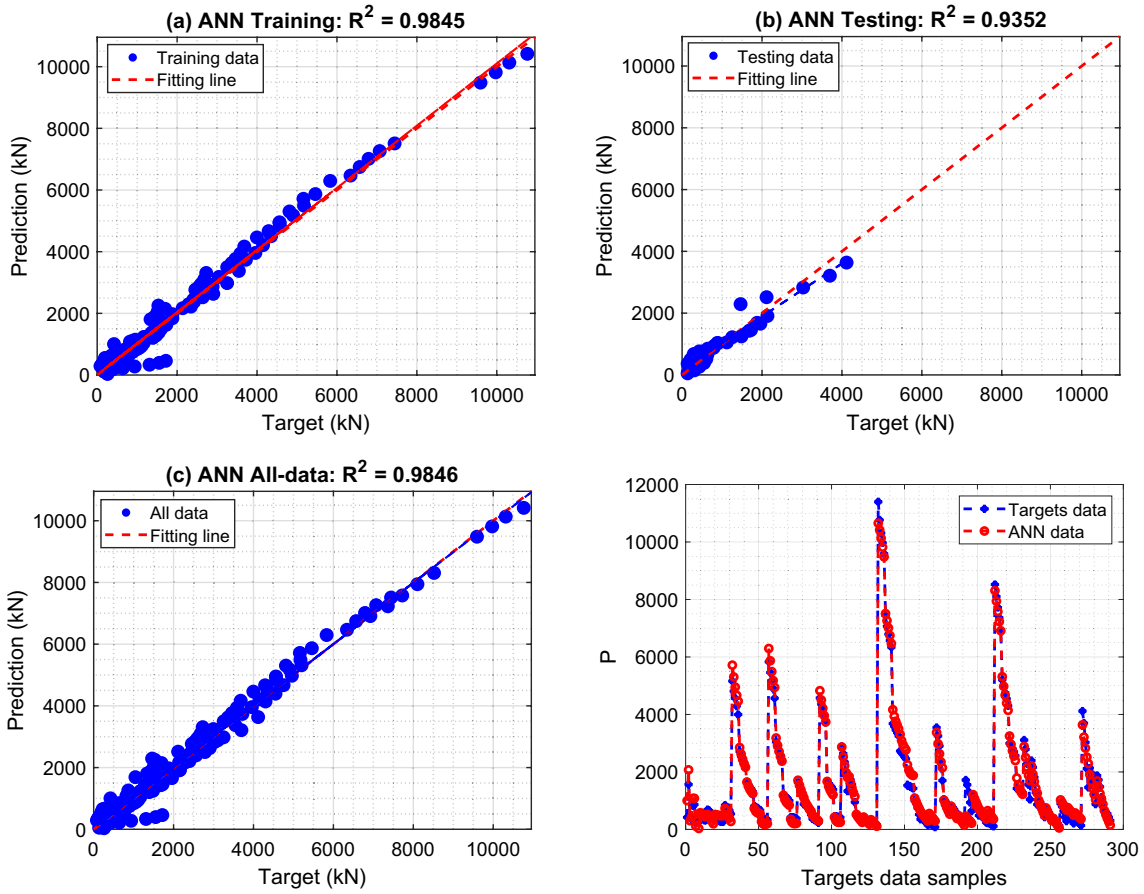

Fig. 10 Performance of ANN model

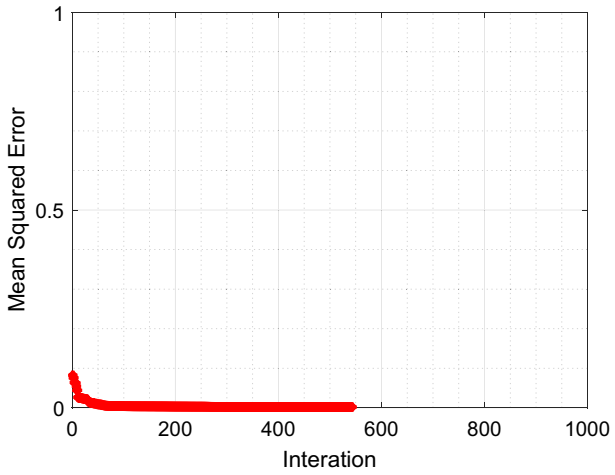

Fig. 11 Convergence process of ANN-PSO model

$$X_n = 2 \times \frac{(X - X_{\min})}{(X_{\max} - X_{\min})} - 1, \tag{9}$$

where X_n is data normalized sample; X, $X_{\max}$, and $X_{\min}$ are the value, maximum, and minimum of the sample under consideration, respectively.

Performance of ML models

Performance indicators

In this study, the predictive performance of three ML models is assessed using R^2, $RMSE$, $MAPE$, and $a20-index$. The determinations of these indexes are expressed as follows:

$$R^2 = 1 - \left(\frac{\sum_{i=1}^{n} (t_i - o_i)^2}{\sum_{i=1}^{n} o_i^2} \right), \tag{10}$$

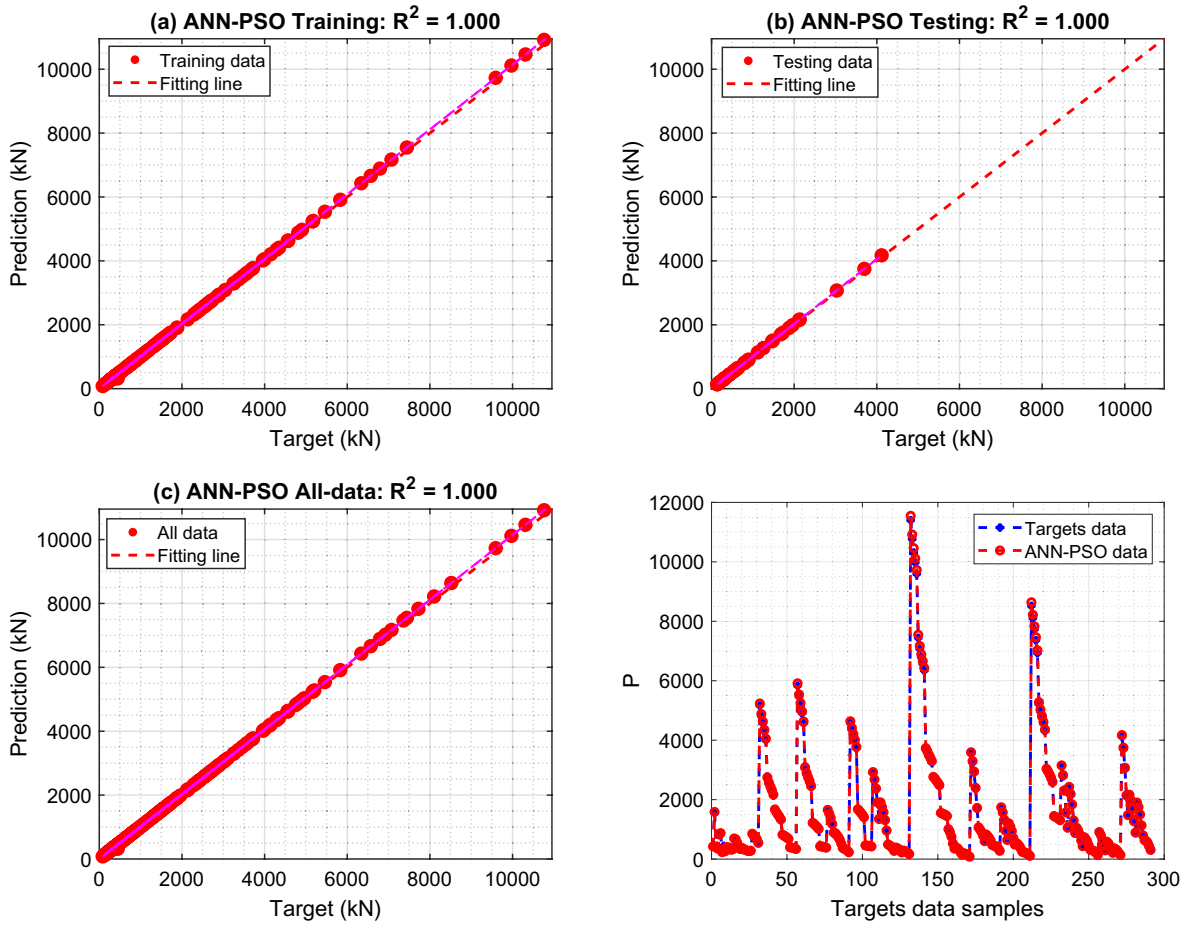

Fig. 12 Performance of ANN-PSO model

$$\text{MAPE} = \frac{1}{n}\sum_{1}^{n}\left(\left|\frac{o_i - t_i}{o_i}\right| \times 100\right), \tag{11}$$

$$\text{RMSE} = \sqrt{\left(\frac{1}{n}\right)\sum_{i=1}^{n}\left(t_i - o_i\right)^2}, \tag{12}$$

$$a20 - \text{index} = \frac{n20}{n}. \tag{13}$$

where t_i is the ith ACC of collected dataset; o_i is the ith ACC of the ML models; n is the number of samples; $n20$ is the number of samples that has a ratio of ACC of collected data and ACC of the ML models range $0.8 - 1.2$.

Performance of GBRT model

Figure 7 and Table 2 show the training, testing, and all datasets performance of GBRT model. It can be seen that the ACC of the cold-formed steel EHS column predicted values of the GBRT model are close to actual values. The R^2, RMSE, MAPE, and $i20 - \text{index}$ values of the GBRT model for training, testing, and all datasets are (0.9989, 0.9980, 0.9988), (65.5810, 85.5038, 69.86) kN, (6.9435, 8.8835, 7.3322)%, and (0.9064, 0.9464, 0.9141), respectively. Moreover, the statistics values (minimum, mean, maximum, standard deviation, and coefficient of variation) of the ratio between predicted and actual values for training, testing, and all datasets are (0.5772, 0.8905, 0.5772), (1.0118, 1.0430, 1.0177), (1.8158, 2.1040, 2.1040), (0.1247, 0.1788, 0.1445), and (0.1331, 0.1715, 0.1419), respectively.

Performance of ANN model

To develop the ANN model, the larger outer diameter (B), smaller outer diameter (D), thickness (t), column length (L), Young's modulus (E), static ultimate tensile strength

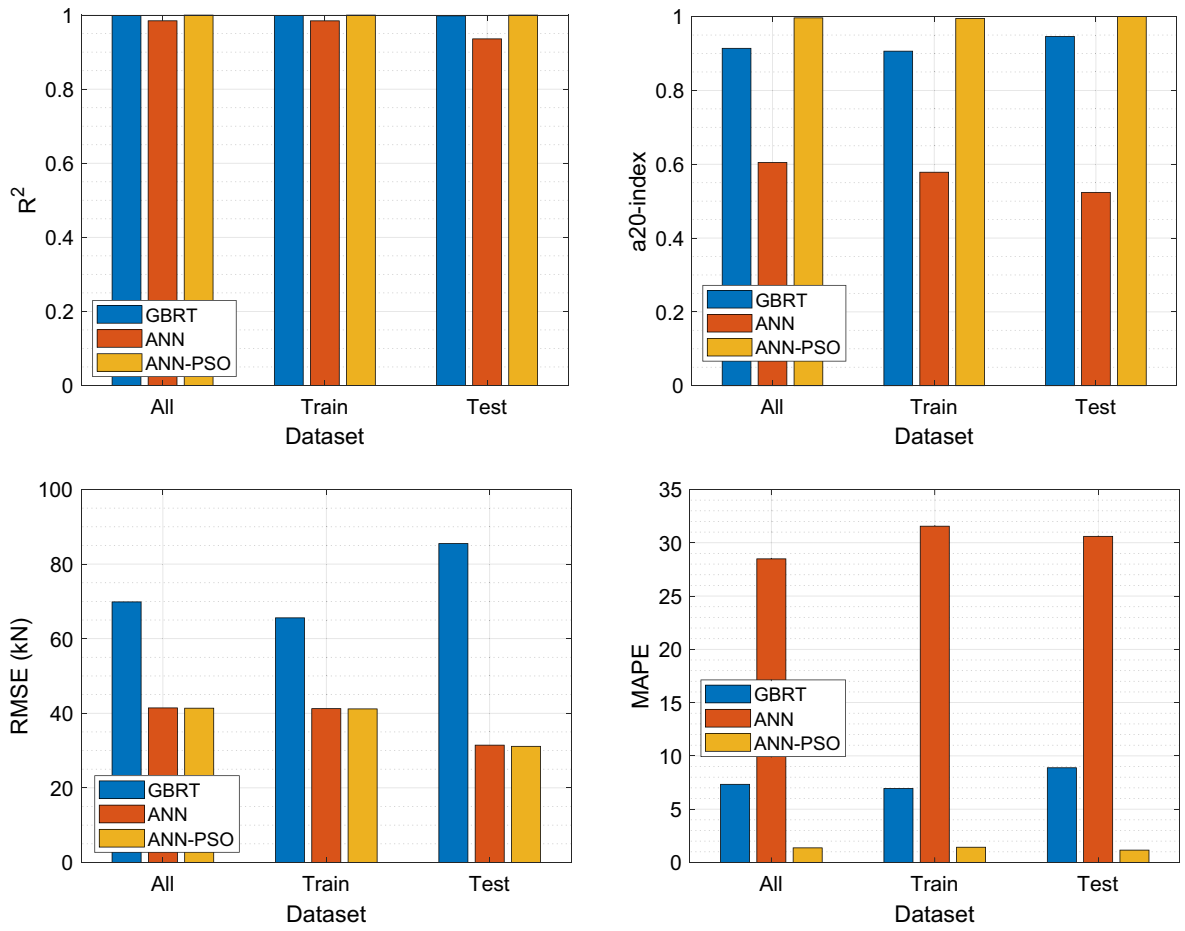

Fig. 13 Comparison of performance metrics between GBTR, ANN, and ANN-PSO models

Fig. 14 The GUI tool for predicting ACC

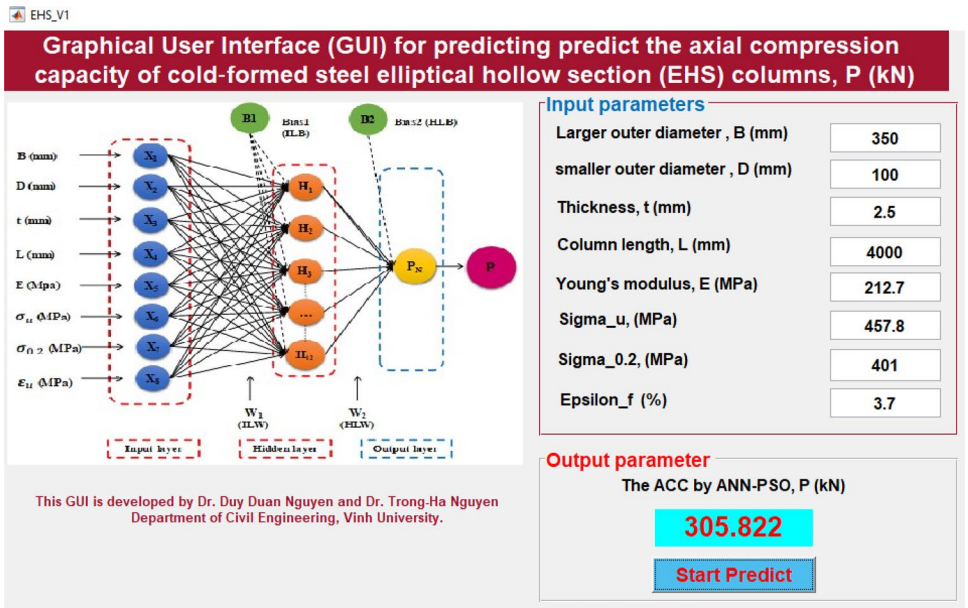

(σ_u), tensile strain fracture (ε_u), and static 0.2% proof stress ($\sigma_{0.2}$) are considered as the input variables, while the ACC of cold-formed steel EHS columns (P) is the output variable.

To obtain the best ANN structure, this study conducts testing of a total of 120 ANN structures with 20 neurons in the hidden layer varied from 1 to 20 and 6 common training rates (0.6, 0.65, 0.70, 0.75, 0.8, 0.85). ANN structures have best-performing as the structures with the highest ranking (i.e., largest R^2 and $i20-$index, smallest RMSE and MAPE). The total ranking matrix of 120 ANN structures is shown in Fig. 8. The best-performing ANN structures have the training, validation, and testing ratios (0.7, 0.15, 0.15), respectively, with 12 hidden layer neurons. Thus, this study uses the ANN structures for predicting the ACC of the cold-formed steel EHS column as shown in Fig. 9:

The training, testing, and all datasets performance of ANN model are shown in Fig. 10 and Table 2. The R^2, RMSE, MAPE, and $i20-$index values of ANN model for training, testing, and all datasets are (0.9845, 0.9358, 0.9846), (41.2368, 31.4530, 41.4337) kN, (31.5565, 30.6033, 28.4896)%, and (0.5784, 0.5238, 0.6048), respectively. Moreover, the statistic values (minimum, mean, maximum, standard deviation, and coefficient of variation) of the ratio between predicted and actual values for training, testing, and all datasets are (0.2815, 0.3825, 0.2815), (1.1300, 0.9862, 1.0759), (7.5511, 2.7003, 7.5511) kN, (0.6856, 0.4353, 0.6093) %, and (0.6067, 0.4414, 0.5664), respectively.

Performance of ANN-PSO model

To develop the ANN-PSO model, the ANN structures with 12 neurons in the hidden layer are used. In this ANN-PSO model, the weights and biases are optimized by the PSO algorithm. The combination technique between the ANN and the PSO algorithm is also shown in Fig. 5.

Figure 11 shows the convergence of the ANN-PSO model after 535 iterations. The MSE optimization value is close to zero. Figure 12 and Table 2 show the training testing, and all datasets performance of ANN-PSO model. The ACC values of the cold-formed steel EHS columns obtained by ANN-PSO are close to actual values (i.e., experimental results). The R^2, RMSE, MAPE, and $i20-$index values of ANN-PSO for training, testing, and all datasets are (1.000, 1.000, 1.000), (41.1693, 31.1362, 41.3631) kN, (1.4281, 1.1583, 1.1583)%, and (0.9951, 1.0000, 0.9966), respectively. Moreover, the statistics values (minimum, mean, maximum, standard deviation, and coefficient of variation) of the ratio between predicted and actual values for training, testing, and all datasets are (0.9808, 0.9858, 0.9808), (0.9896, 0.9884, 0.9890), (1.3882, 0.9977, 1.3882), (0.0281, 0.0026, 0.0236), and (0.0284, 0.0026, 0.0239), respectively.

Comparison of GBRT, ANN, and ANN-PSO models

Figure 13 shows the bar plots of the R^2, RMSE, MAPE, and $i20-$index of the training, testing, and all datasets from predicted results obtained by GBTR, ANN, and ANN-PSO. This result shows that the ANN-PSO model outperforms GBRT and ANN models in predicting the ACC of the cold-formed steel EHS columns. Specifically, the R^2 and $i20-$index are close to 1.0, and RMSE and MAPE are smallest for the ANN-PSO model.

Table 2 shows the statistical values of the ratio between predicted and actual values for all datasets. The mean value of ANN-PSO is close to 1.0, implying that the ANN-PSO model is better than the GBRT and ANN models for predicting ACC of the EHS column.

Obviously, ANN-PSO is the optimal model compared to GBRT and ANN for estimating ACC of the steel EHS column. Thus, for the convenience of engineers' practice, a new graphical user interface (GUI) tool based on the ANN-PSO was built, which is shown in Fig. 14. This tool is provided freely at https://github.com/duyduan1304/GUI_EHS. When using the GUI tool, it should be noted that the ANN-PSO model only predicts results within the range of input data (i.e., from the minimum to the maximum).

Conclusions

This study successfully develops GBRT, ANN, and ANN-PSO models for predicting ACC of the cold-formed steel EHS column based on the 291 datasets. The predictive performance of GBRT, ANN, and ANN-PSO models is evaluated using R^2, RMSE, MAPE, and $i20-$index indicators. The following conclusions are obtained.

- Three developed ML models (GBRT, ANN, and ANN-PSO) predict the ACC of cold-formed steel EHS columns accurately.
- ANN-PSO has the most efficient performance with $R^2 = 1.00$, RMSE $= 41.3631$, MAPE $= 1.3689$, and $i20-$index $= 0.9966$ compared to GBRT and ANN models.
- A GUI tool based on the ANN-PSO model is built for the convenience of design practices.

Author contributions T-HN conceptualization, software, visualization, writing—original draft. D-XN methodology, data curation. T-TTN validation; visualization. V-LP validation; visualization. D-DN methodology, formal analysis, writing—original draft, writing—review and editing, supervision.

Funding No funding was used in this study.

Data availability The data used to support the findings of this study are included in the article.

Declarations

Conflict of interest The authors declare that they have no known competing financial interests or personal relationships that could have appeared to influence the work reported in this paper.

References

1993-3-1 E. (2006). Eurocode 3: Design of steel structures—Part 3–1. In: The European Union Per Regulation 305/2011.

AISI-S100. (2016). *North American Specification for the Design of Cold-Formed Steel Structural Members*. American Iron and Steel Institute.

Alizamir, M., & Sobhanardakani, S. (2018). An artificial neural network-particle swarm optimization (ANN-PSO) approach to predict heavy metals contamination in groundwater resources. *Jundishapur Journal of Health Sciences*, *10*(2).

Alzoubi, I., Delavar, M. R., Mirzaei, F., & NadjarArrabi, B. (2018). Comparing ANFIS and integrating algorithm models (ICA-ANN, PSO-ANN, and GA-ANN) for prediction of energy consumption for irrigation land leveling. *Geosystem Engineering, 21*(2), 81–94.

ANSI, AISC360. (2016). *Specification for Structural Steel Buildings*. American Institute of Steel Construction.

Chan, T. M., & Gardner, L. (2009). Flexural buckling of elliptical hollow section columns. *Journal of Structural Engineering, 135*(5), 546. https://doi.org/10.1061/(ASCE)ST.1943-541X.0000005.

Chen, M.-T., & Young, B. (2019a). Behavior of cold-formed steel elliptical hollow sections subjected to bending. *Journal of Constructional Steel Research, 158*, 317–330.

Chen, M.-T., & Young, B. (2019b). Material properties and structural behavior of cold-formed steel elliptical hollow section stub columns. *Thin-Walled Structures, 134*, 111–126.

Chen, M.-T., & Young, B. (2019c). Structural performance of cold-formed steel elliptical hollow section pin-ended columns. *Thin-Walled Structures, 136*, 267–279.

Chen, M.-T., & Young, B. (2020). Beam-column tests of cold-formed steel elliptical hollow sections. *Engineering Structures, 210*, 109911.

Dias, J., & Silvestre, N. (2011). A neural network based closed-form solution for the distortional buckling of elliptical tubes. *Engineering Structures, 33*(6), 2015–2024.

Eberhart, R. C., Shi, Y., & Kennedy, J. (2001). *Swarm intelligence*. Elsevier.

Friedman, J. H. (2001). Greedy function approximation: a gradient boosting machine. *Annals of Statistics*. https://doi.org/10.1080/15567036.2019.1630521.

Golafshani, E. M., & Ashour, A. (2016). A feasibility study of BBP for predicting shear capacity of FRP reinforced concrete beams without stirrups. *Advances in Engineering Software, 97*, 29–39.

Hao, X., Hu, X., Liu, T., Wang, C., & Wang, L. (2022). Estimating urban PM2.5 concentration: An analysis on the nonlinear effects of explanatory variables based on gradient boosted regression tree. *Urban Climate, 44*, 101172. https://doi.org/10.1016/j.uclim.2022.101172.

Kaveh, A. (2014). *Advances in metaheuristic algorithms for optimal design of structures*. Springer.

Kaveh, A., & Bondarabady, H. R. (2004). Wavefront reduction using graphs, neural networks and genetic algorithm. *International Journal for Numerical Methods in Engineering, 60*(11), 1803–1815.

Kaveh, A., Gholipour, Y., & Rahami, H. (2008). Optimal design of transmission towers using genetic algorithm and neural networks. *International Journal of Space Structures, 23*(1), 1–19.

Kumar, C. V., Sargunan, K., Vasa, J., Jesuraj, V. P., Punitha, A., & Karthikeyan, R. (2022). Applying ANN–PSO algorithm to maximize the compressive strength and split tensile strength of blended self curing concrete on the impact of supplementary cementitious materials. *International Journal on Interactive Design and Manufacturing (IJIDeM)*. https://doi.org/10.1007/s12008-022-00907-z.

Law, K., & Gardner, L. (2013). Global instability of elliptical hollow section beam-columns under compression and biaxial bending. *International Journal of Steel Structures, 13*(4), 745–759.

Le, L. T., Nguyen, H., Dou, J., & Zhou, J. (2019). A comparative study of PSO-ANN, GA-ANN, ICA-ANN, and ABC-ANN in estimating the heating load of buildings' energy efficiency for smart city planning. *Applied Sciences, 9*(13), 2630.

Liu, J., Jiang, Y., Han, W., & Sakaguchi, O. (2021). Optimized ANN model for predicting rock mass quality ahead of tunnel face using measure-while-drilling data. *Bulletin of Engineering Geology and the Environment, 80*(3), 2283–2305.

Manna, S., Biswas, S., Kundu, R., Rakshit, S., Gupta, P., & Barman, S. (2017). A statistical approach to predict flight delay using gradient boosted decision tree. In: *2017 International conference on computational intelligence in data science (ICCIDS)*.

Mohammed, A., & Cashell, K. A. (2021). Cross-sectional behaviour and design of ferritic and duplex stainless steel EHS in compression. *Steel Construction, 14*(4), 279–287. https://doi.org/10.1002/stco.202100001.

Naser, M., Thai, S., & Thai, H.-T. (2021). Evaluating structural response of concrete-filled steel tubular columns through machine learning. *Journal of Building Engineering, 34*, 101888. https://doi.org/10.1016/j.jobe.2020.101888.

Nguyen, D.-D., & Nguyen, T.-H. (2023). GBRT-based model for predicting the axial load capacity of the CFS-SOHS columns. *Asian Journal of Civil Engineering*. https://doi.org/10.1007/s42107-023-00743-w.

Nguyen, D.-D., Tran, N.-L., & Nguyen, T.-H. (2023). ANN-based model for predicting the axial load capacity of the cold-formed steel semi-oval hollow section column. *Asian Journal of Civil Engineering, 24*(5), 1165–1179.

Nikbin, I. M., Rahimi, S., & Allahyari, H. (2017). A new empirical formula for prediction of fracture energy of concrete based on the artificial neural network. *Engineering Fracture Mechanics, 186*, 466–482. https://doi.org/10.1016/j.engfracmech.2017.11.010.

Patel, V. M., & Mehta, H. B. (2018). Thermal performance prediction models for a pulsating heat pipe using artificial neural network (ANN) and regression/correlation analysis (RCA). *Sādhanā, 43*(11), 1–16. https://doi.org/10.1007/s12046-018-0954-3.

Prettenhofer, P., & Louppe, G. (2014). Gradient boosted regression trees in scikit-learn. PyData 2014

Qi, C., Fourie, A., & Zhao, X. (2018). Back-analysis method for stope displacements using gradient-boosted regression tree and firefly algorithm. *Journal of Computing in Civil Engineering, 32*(5),

04018031. https://doi.org/10.1061/(ASCE)CP.1943-5487.0000779.

Rönnholm, M., Arve, K., Eränen, K., Klingstedt, F., Salmi, T., & Saxén, H. (2005). ANN modeling applied to NO X reduction with octane. A nn future in personal vehicles. *Adaptive and Natural Computing Algorithms* (pp. 100–103). Springer. https://doi.org/10.1007/3-211-27389-1_24.

Shariati, M., Mafipour, M. S., Mehrabi, P., Bahadori, A., Zandi, Y., Salih, M. N., & Poi-Ngian, S. (2019). Application of a hybrid artificial neural network-particle swarm optimization (ANN-PSO) model in behavior prediction of channel shear connectors embedded in normal and high-strength concrete. *Applied Sciences, 9*(24), 5534.

Soltani, H., Karimi, A., & Falahatpisheh, S. (2022). The optimization of biodiesel production from transesterification of sesame oil via applying ultrasound-assisted techniques: Comparison of RSM and ANN–PSO hybrid model. *Chemical Product and Process Modeling, 17*(1), 55–67.

Theofanous, M., Chan, T. M., & Gardner, L. (2009). Structural response of stainless steel oval hollow section compression members. *Engineering Structures, 31*(4), 922–934.

Toghyani, S., Ahmadi, M. H., Kasaeian, A., & Mohammadi, A. H. (2016). Artificial neural network, ANN-PSO and ANN-ICA for modelling the Stirling engine. *International Journal of Ambient Energy, 37*(5), 456–468.

Tran, N.-L., Nguyen, D.-D., & Nguyen, T.-H. (2022). Prediction of speed limit of cars moving on corroded steel girder bridges using artificial neural networks. *Sādhanā, 47*(3), 1–14.

Tran, N.-L., Nguyen, T.-H., Phan, V.-T., & Nguyen, D.-D. (2021). A machine learning-based model for predicting atmospheric corrosion rate of carbon steel. *Advances in Materials Science and Engineering*. https://doi.org/10.1155/2021/6967550.

Tran, V.-L., & Kim, S.-E. (2020). Efficiency of three advanced data-driven models for predicting axial compression capacity of CFDST columns. *Thin-Walled Structures, 152*, 106744.

Tran, V.-L., Thai, D.-K., & Kim, S.-E. (2019). Application of ANN in predicting ACC of SCFST column. *Composite Structures, 228*, 111332. https://doi.org/10.1016/j.compstruct.2019.111332.

Yao, Y., Quach, W.-M., & Young, B. (2019). Cross-section behavior of cold-formed steel elliptical hollow sections—A numerical study. *Engineering Structures, 201*, 109797. https://doi.org/10.1016/j.engstruct.2019.109797.